Quantum soliton dynamics in vibrational chains: Comparison of fully correlated, mean field, and classical dynamics

Daniel Neuhauser
Chemistry and Biochemistry Department, University of California, Los Angeles, California 90095-1569

Roi Baer and Ronnie Kosloff
Department of Physical Chemistry, Hebrew University, Jerusalem, 91904, Israel

(Received 4 October 2002; accepted 8 January 2003)

The dynamics of a chain of vibrational bonds which develop a classical solitary compression wave is simulated. A converged fully correlated quantum mechanical calculation is compared with a time dependent mean field approach (TDSCF) and with a classical simulation. The dynamics were all generated from the same Hamiltonian. The TDSCF and classical calculations show a fully developed solitary wave with the expected dependence of group velocity on amplitude. The full quantum calculations show a solitary-like wave which propagates for a while but then degrades. The robustness of the compression wave depends on the initial preparation. Evidence of partial recurrence of the wave has also been observed. © *2003 American Institute of Physics.*
[DOI: 10.1063/1.1555797]

I. INTRODUCTION

Fermi, Pasta, and Ulam[1] pioneered the numerical study of dynamics of a coupled chain of nonlinear oscillators and in particular the issue of energy redistribution. The surprising effect was that energy distribution was slow and that some collective modes of the system persist for very long times. These studies were extended by Toda[2] who found nontrivial integrable wavelike solutions for such systems of coupled oscillators. These waves are closely related to the nonlinear solitary wave phenomena. Rolfe, Rice, and Dancz[3,4] have studied the characters of solitary waves in a periodic chain of coupled oscillators. They found both classically and semiclassically that the phenomena is rather general and that almost any potential with a steep repulsion wall will support compression solitary waves. A simple reasoning is based on the fact that by compressing the bond the frequency of local oscillation increases, thus increasing the group velocity of the compression wave. The outcome is a wave that creates its own propagating environment. The signature of this type of wave is that its group velocity increases with amplitude. Once created it moves around the chain with almost no loss or change of shape.

The quantum analog of such motion is a subtle issue. Strictly speaking the linearity of quantum mechanics means that it cannot support such nonlinear phenomena. Nevertheless it is clear that for short times solitary like waves analogous to their classical counterparts will propagate. Eventually these waves will lose their correspondence with their classical counterparts when the quantum-classical analogy breaks down.[5,6]

The most common approach of modeling a quantum many-body problem is by employing the mean field approximation. This approach has been applied to transport of vibrational energy in proteins by Davidov[7,8] where the problem was cast into a nonlinear Schrödinger equation. The approximation supports solitary wave solution. Solitary solutions were also found for the mean field Gross–Pitevskii model for Bose–Einstein condensates.[9]

In this paper we examine quantum solitary-like compression waves in molecular dynamics, specifically in polymer chains. The motivation beyond studying solitons is that they can have several interesting properties. First, they are very stable to disturbances. Furthermore, they can be used to examine the properties of the medium they are at. For example, for a system with chromophores, one can imagine exciting a chromophore on one side with a strong oscillation, injecting a soliton, which then propagates undisturbed (or only slightly disturbed) towards the other chromophores. The time at which it arrives at the other chromophores can be timed giving an indication of the distance between the chromophores. Further, the soliton arrival time is a gauge of the properties of the medium in between the chromophores.

This paper examines the properties of soliton in 1D systems on two levels. First, we examine, in a fully correlated model, the stability of the solitons and the dependence of their group velocity on soliton amplitude. Due to the steep increase in cost of the calculation the study is done for a limited system size (8 periodic sites). We then study the relation of the exact numerical solution describing the quantal soliton to approximate models. For this purpose we compare fully-correlated (CI), time-dependent self-consistent field (TDSCF), and classical simulations (Cls). In brief, the results are that TDSCF and classical simulations are different (in the model) by 10–20%, but give a similar dependence of the soliton amplitude on initial excitation. Thus, it is feasible to determine soliton motion for large systems by approximate methods.

The paper is arranged as follows: Section II has the methodology; results are presented in Sec. III; and Sec. IV concludes.

II. METHODOLOGY

The system studied is of a periodic 1D vibrational lattice (Toda lattice), with the Hamiltonian,[6]

$$H=\sum_{j=1}^{N}\frac{p_j^2}{2m}+\sum_{j=1}^{N}v(x_{j+1}-x_j), \tag{2.1}$$

where we introduced the atomic positions momenta, the (identical) atomic mass, and the one-body vibrational potential. We assume periodic boundary conditions, so in the potential term the x_{N+1} refers to x_1. The potential term has a Toda (Morse) form,[2,6,10,11]

$$v(u)=D_0\left(e^{-(u-r_0)/\sigma_0}+\frac{(u-r_0)}{\sigma_0}-1\right), \tag{2.2}$$

where r_0 is the equilibrium distance, u is the distance between the particles, and σ_0 is the range of the potential.

The Hamiltonian was studied with three approaches.

A. Fully-correlated basis-set approach (quantum-CI)

In this approach the full time-dependent wave function is expanded in the vibrational coordinate

$$\Psi(\mathbf{x},t)=\sum_{\mathbf{n}}a_{\mathbf{n}}(t)\phi_{n_1}(x_1)\cdots\phi_{n_N}(x_N), \tag{2.3}$$

where

$$\mathbf{x}\equiv\mathbf{x_1},\mathbf{x_2},\ldots,\mathbf{x_N},$$
$$\mathbf{n}\equiv\mathbf{n_1},\mathbf{n_2},\ldots,\mathbf{n_N}, \tag{2.4}$$

and we introduced the one-body basis functions, which are constructed as eigenstates of a zeroth-order noninteracting Hamiltonian,

$$\hat{\mathbf{H}}_\mathbf{0}\phi_j(x_j)=\left(\frac{p^2}{2m}+v_0(x_j)\right)\phi_j(x_j)=\epsilon_j\phi_j(x_j), \tag{2.5}$$

and where we introduced the one body vibrational potential $v_0(x_j)=(\kappa/2)(x_j-r_0)^2$ associated with the zeroth-order Hamiltonian and associated eigenvalues.

The Hamiltonian becomes a simple sparse matrix in this vibrational representation. The diagonal element is

$$H_{\mathbf{n};\mathbf{n}}=\sum_j\langle\phi_{n_j}|\frac{p_j^2}{2m}|\phi_{n_j}\rangle+\sum_j v^j_{n_j,n_{j+1},n_j,n_{j+1}}, \tag{2.6}$$

where

$$v^j_{k,l,m,n}\equiv\langle\phi_k\phi_l|v(x_{j+1}-x_j)|\phi_m\phi_n\rangle. \tag{2.7}$$

The only nonzero off-diagonal elements are nearest neighbor ones. Specifically given **n** Eq. (2.4), and **k** the same as **n** except for $k_j\neq n_j$, then

$$H_{\mathbf{k};\mathbf{n}}=\langle\phi_{k_j}|\frac{p_j^2}{2m}|\phi_{n_j}\rangle+v^{j-1}_{n_{j-1},k_j,n_{j-1},n_j}+v^j_{k_j,n_{j+1},n_j,n_{j+1}}. \tag{2.8}$$

The second case is for $k_j\neq n_j$ and $k_{j+1}\neq n_{j+1}$ then

$$H_{\mathbf{k};\mathbf{n}}=v^j_{k_j,k_{j+1},n_j,n_{j+1}}, \tag{2.9}$$

where these expressions are cyclic in j (i.e., $j+1\equiv 1$ when $j=N$, etc.).

The expansion of the wave function is limited numerically by two simple criteria; finiteness of the expansion in each dimension

$$0\leqslant n_j<n_{\max}, \tag{2.10}$$

and an energy criteria

$$H_{\mathbf{n};\mathbf{n}}\leqslant E_{\max}, \tag{2.11}$$

where $n_{\max}$ and $E_{\max}$ are numerical convergence parameters.

The locally based expansion can pose a problem since the soliton is nonsymmetric with a different frontal (pushing) and backward (pulling) profile. Therefore, after a soliton passes a component of the vibrational lattice, the lattice point are expected to be translationally shifted even though they start and end with zero momentum. This is similar to a mechanism whereby a falling cat does a rotational shift and ends up on its feet. The difficulty is caused by the finite basis-set representation of the wave function which is not translationally invariant, i.e., the quality of the basis set expansion degrades when one adds a large shift to the coordinates. The basis set is optimized for vibrations around the equilibrium particle points. In the present simulation this problem is overcome by employing a pair of counterpropagating solitons, so any vibrational shift of the coordinates by a passing soliton is negated at later times by the other soliton. Although the Hamiltonian seems simpler in bond coordinates it is more difficult to impose the constraint that $\Sigma_j u_j=0$ (periodic condition) i.e., the sum of bond-coordinates is zero (modulus the ring length). For this reason atomic positions were used.

There are two possible approaches to define the initial wave function Ψ_0. In the first, it is determined as a coherent state with a specific position and momentum in each dimension, as follows: We choose classical initial coordinates, $\overline{x_j}$ so that the bonds, defined as

$$u_j=\overline{x}_{j+1}-\overline{x}_j,$$
$$u_N=\overline{x}_1-\overline{x}_N, \tag{2.12}$$

are essentially distributed as a Gaussian compression wave,

$$u_j=-\overline{u}\exp\left(-\frac{(j-j_0)^2}{2w^2}\right)+\text{const.} \tag{2.13}$$

The constant is determined from the requirement that $\Sigma_j u_j=0$, and the width of the compression wave is typically $w=\sqrt{2}$. The magnitude of the compression wave is determined by $\overline{u}$ and j_0 is the atom at the center of the initial compression wave.

The classical initial position (and vanishing initial momentum) determine the initial coherent state in each dimension. For each atom j we then determine a coherent state $\zeta_j(x)$ based on the initial $\overline{x_j}$, and determine its coefficient

$$\zeta_j=c_j\sum_{n=0}^{n_{\max}-1}b_{jn}\phi_n(x_j), \tag{2.14}$$

where the general coherent state (for general v_0) is $b_{jn} = \langle \phi_n | \exp(-ip\overline{x_j}) | \phi_0 \rangle$. In this example we chose v_0 to be harmonic, so the ϕ_n are harmonic oscillator eigenstates with the associated analytic expression for b_{jn}. The total initial wave function is finally determined as[10,11]

$$a_{\mathbf{n}} = \prod_j b_{jn_j}. \tag{2.15}$$

The second approach for initiating the dynamics aims to physically mimic the way that a soliton is created. The initial step is to relax the chain. This is done with an imaginary-time propagation [i.e., acting with $\exp(-H\tau)$] with τ sufficiently large, using a standard Chebychev propagation.[12] After that, a force is applied for a short time on one atom. In practice, one adds to the Hamiltonian a term $-f(t)x_1$, where f is the force (of constant magnitude f_0 up to time t_f, and zero afterwards) and x_1 is the coordinate of the first atom (where the pushing is applied). This term gives rise, in the basis-set picture, to the following addition to H:

$$H_{\mathbf{k};\mathbf{n}} \rightarrow H_{\mathbf{k};\mathbf{n}} - f(t) \langle \phi_{k_1} | x_1 | \phi_{n_1} \rangle \Pi_j = 2^N \delta_{k_j n_j}.$$

The two choices of the initial wave packet have their pros and cons. The initial coherent state is intimately analogous to a classical description; however, the second choice, of a relaxed initial state, leads to damping of contributions which are unrelated to the soliton, thereby allowing a cleaner soliton.

With either of the choices to start the dynamics, the initial wave function is then propagated forward in (real) time using the Chebychev propagation[13] with the sparse Hamiltonian.

The average one-body position (and analogously the momentum) are then plotted as a function of time,

$$\langle x_j \rangle \equiv \langle \Psi_0 | x_j | \Psi_0 \rangle = \sum_{k_j n_j} x_{j;k_j,n_j} \rho_{j;n_j,k_j}, \tag{2.16}$$

where

$$\rho_{j,k_j,n_j} = \sum_{n_1,n_2,\ldots,n_{j-1},n_{j+1},\ldots,n_N} a^*_{n_1,n_2,\ldots,n_{j-1},n',n_{j+1},\ldots,n_N} \times a_{n_1,n_2,\ldots,n_{j-1},n,n_{j+1},\ldots,n_N}, \tag{2.17}$$

$$x_{j;k_j,n_j} = \int \phi^*_{k_j}(x_j) x_j \phi_{n_j}(x_j) dx_j. \tag{2.18}$$

B. Time dependent self-consistent field approximation (quantum-TDSCF)

Self consistent mean field approximations are common in many body problems. In a time dependent framework for multimode molecular systems the method is well developed.[14,15] For the system of coupled oscillators the associated equations are

$$\Psi(\mathbf{x},t) = \prod_j \zeta_j(x_j,t), \tag{2.19}$$

where the time-dependent individual functions are determined from

$$i\hbar \frac{\partial \zeta_j}{\partial t} = h_j \zeta_j, \tag{2.20}$$

with the local mean field Hamiltonian,

$$h_j = \frac{p^2}{2m} + \int v(x_{j+1} - x_j) |\zeta(x_{j+1})|^2 dx_{j+1} + \int v(x_j - x_{j-1}) |\zeta(x_j)|^2 dx_{j-1}. \tag{2.21}$$

This equation is solved also by expanding ζ_j into a sum over vibrational eigenstates with standard Runge–Kutta time-propagation. The initial wave function is the same as in the full-CI approach, and the average position and momentum as a function of time are trivially determined from $\zeta_j(x_j,t)$.

C. Classical simulations

Classical simulations are run by integrating the Hamilton equations of motion generated from the Hamiltonian (2.1). The initial conditions are given by $x_{\text{classical},j}(t=0) = \overline{x_j}$.

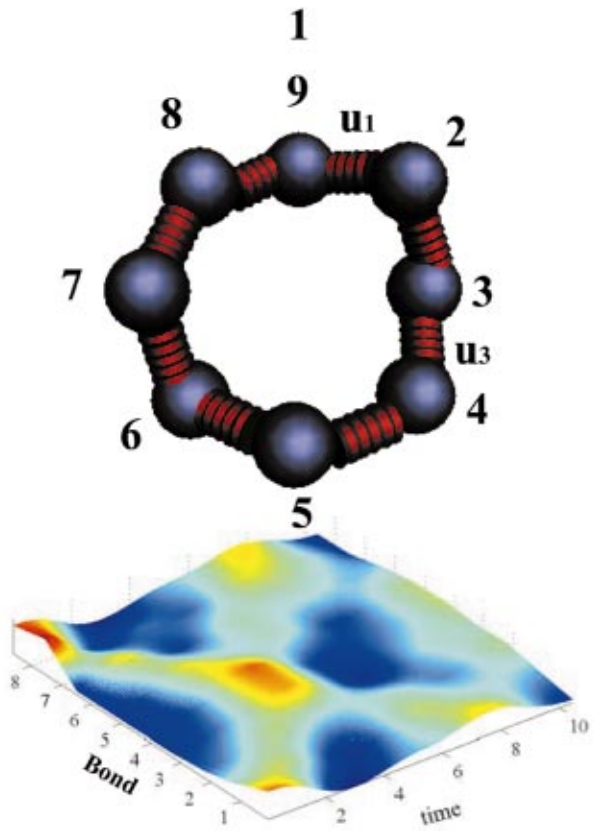

FIG. 1. (Color) Schematic model of the lattice and the bond displacement as a function of time. In the sterioscopic projection the compression regions are shown as ridges. Two compression waves are produced starting from particle 1 ($\overline{u}=1$). The plot is produced by interpolating the value of the amplitudes on each bond.

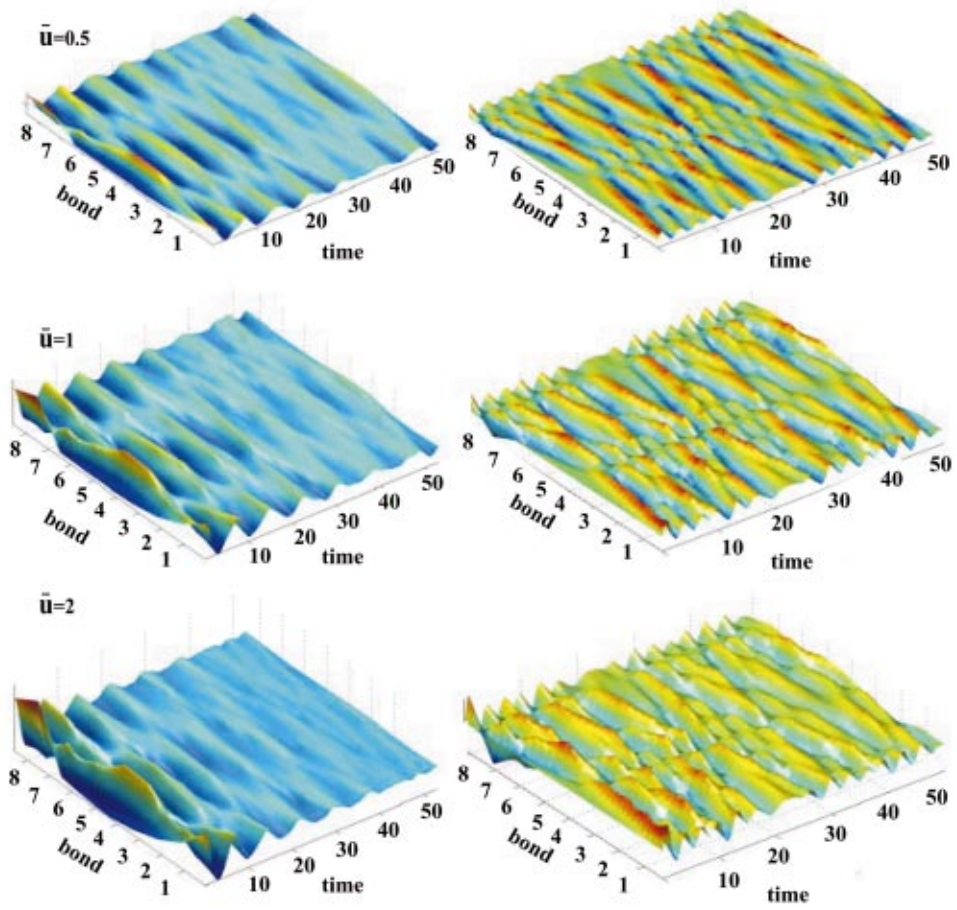

FIG. 2. (Color) Comparing the compression wave propagation on a periodic structure composed of eight particles for the different initial conditions for the quantum-CI calculation. The left panels show the classical-like initial conditions. The right panels show the impulsive initial conditions. The group velocity of the initial state with $\bar{u}_1=0.5$ was $v_g=1.15$ for $\bar{u}_1=1$, $v_g=1.12$ and for $\bar{u}_1=2$, $v_g=1.3$.

III. RESULTS

The first set of simulations was on a small periodic system, with $N=8$ atoms. The parameters used were

$$\hbar=1,\ m=1,\ D_0=1,\ \sigma_0=1,\ r_0=0.5,\ \kappa=1,$$

where r_0 is immaterial for the true fully-correlated dynamics and just shifts the equilibrium bond distance.

For this system a converged quantum calculation is possible therefore it serves as benchmark for the TDSCF and classical approximations.

Figure 1 shows a schematic view of the system and the bond displacements as a function of time. The calculation presents the quantum-CI results where the bond distance in the wave function is defined as in Eq. (2.12),

$$u_j=\langle x_{j+1}\rangle-\langle x_j\rangle.$$

The wave is initiated by compressing bond 1. It then propagates simultaneously to both sides of the chain. At time $t=4$ the compression wave collides at bond 4. The waves survive the collision and the two compression waves proceed on until the next collision.

Figure 2 compares the propagating waves initiated by two set of initial preparations for three initial conditions for the displacement, $\bar{u}=0.5$, 1, 2. The group velocity increases with amplitude which is in accordance with their solitary character. The two waves propagate and wrap around due to the periodic boundary conditions. The waves are seen to survive at least 10 revolutions, but their amplitude seems to decrease, indicating that the solitary character is degraded.

The compression wave generated by the impulsive initial condition is more robust. The solitary-like wave survives for a longer period than the one generated from the classical initial conditions. Figure 3 shows a longer time propagation for $\bar{u}=2$. The compression waves show a partial revival pattern after 80 time units.

Figure 4 is a comparison of the bond displacement for the full CI calculation the approximated TDSCF, and the classical calculation Cls. The TDSCF equations are nonlin-

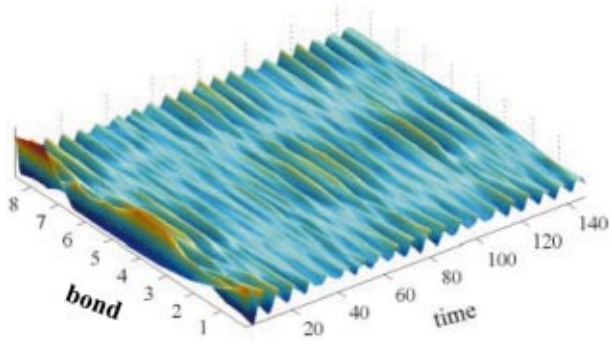

FIG. 3. (Color) Quantum-CI calculation for longer propagation time with classical-like initial conditions showing recursions ($\bar{U}=2$).

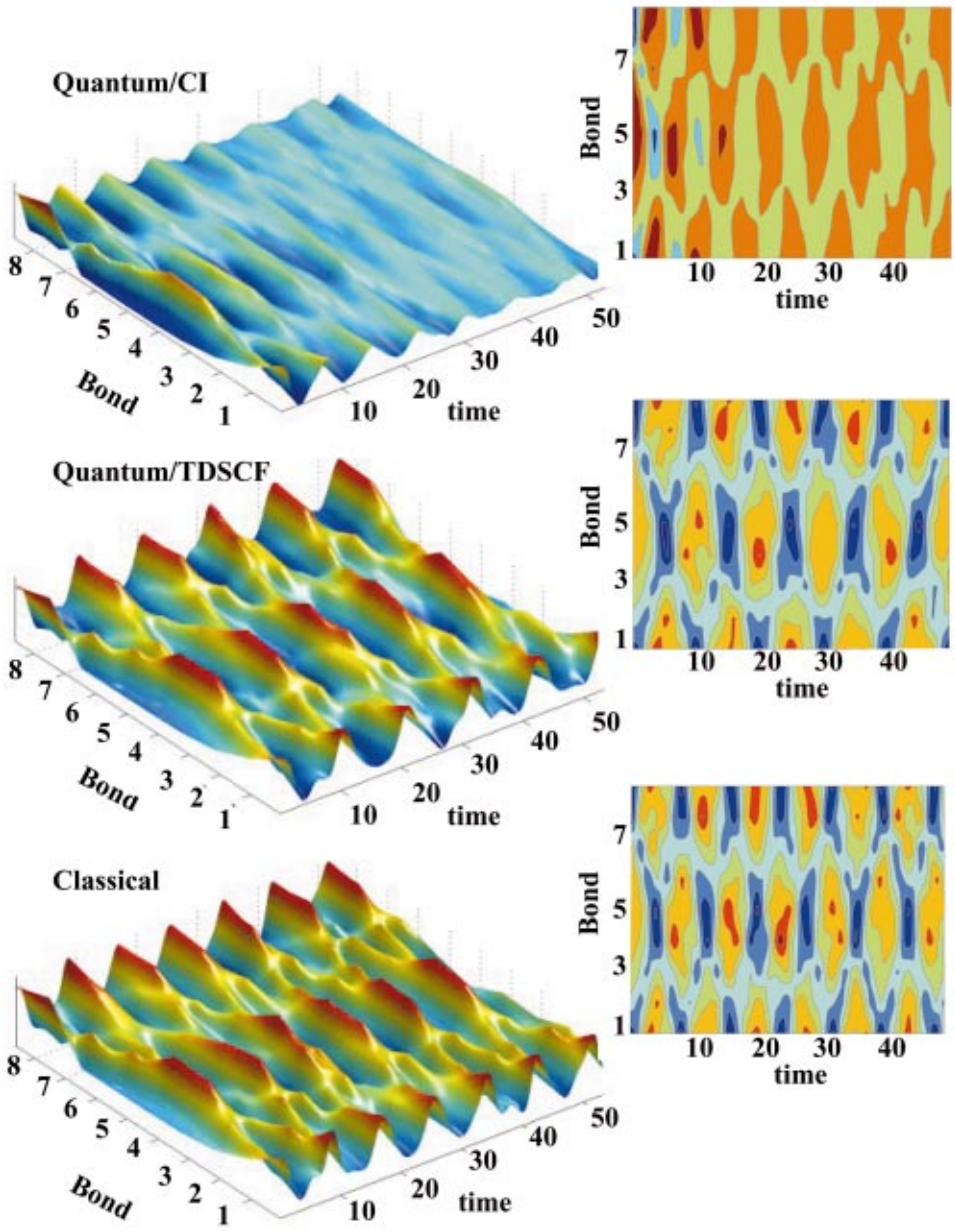

FIG. 4. (Color) Comparing the compression wave propagation on a periodic structure composed of eight bonds for the same initial conditions for the quantum-CI calculation, quantum-TDSCF calculation, and the classical calculation-Cls. The initial displacement is $\overline{U}=0.5$. The right panel shows a stereoscopic projection and the left panel shows a colored contour map. The blue color indicates regions of compression.

ear, so it is not surprising that the soliton survives for indefinitely many oscillations. The soliton survives intact the periodic collisions with the opposite solitary wave.

The results of Figs. 2 and 3 are quantified in Fig. 7, which shows that the velocity of the waves (estimated from the time it takes the soliton to re-encounter) is a rising function of its amplitude.

The TDSCF and the fully-correlated results are similar at very short-times, as expected. Later, the group velocity in the TDSCF is slower than the fully-correlated approach. A possible reason for the difference in group velocity is that the TDSCF approximation is coordinate dependent. The optimal coordinates for the mean field TDSCF are those which minimize the correlation, i.e., the normal coordinates of the chain a choice adopted by Dancz and Rice.[3] The classical-like local atomic coordinates are not optimal for describing the motion.

Interestingly, there is another hint of soliton behavior in the full-CI study of Fig. 4, as the primary soliton wave is accompanied by regular, slower waves. This is much more evident in Fig. 5, which shows the TDSCF results for a much larger chain (with 64 atoms) where the slow wave which accompanies each soliton is clear. The speed of that wave does not increase with soliton speed.

The classical and the TDSCF results are similar but not identical (cf. Figs. 5 and 6). The TDSCF wave is more robust and has a slower group velocity. We have also studied the soliton behavior as a function of the quantum nature of the problem, i.e., of $\hbar$. Figure 7 shows the velocity-amplitude relation for both TDSCF with several values of $\hbar$ (1 and 2) as well as the classical results. Interestingly, the TDSCF results do not match the classical results even in the limit of $\hbar$ small. For the normal coordinate TDSCF, Dancz and Rice[3] were able to map the quantum TDSCF propagation to a classical one with softer scaled parameters. This is in agreement with the slower group velocity found in the present TDSCF.

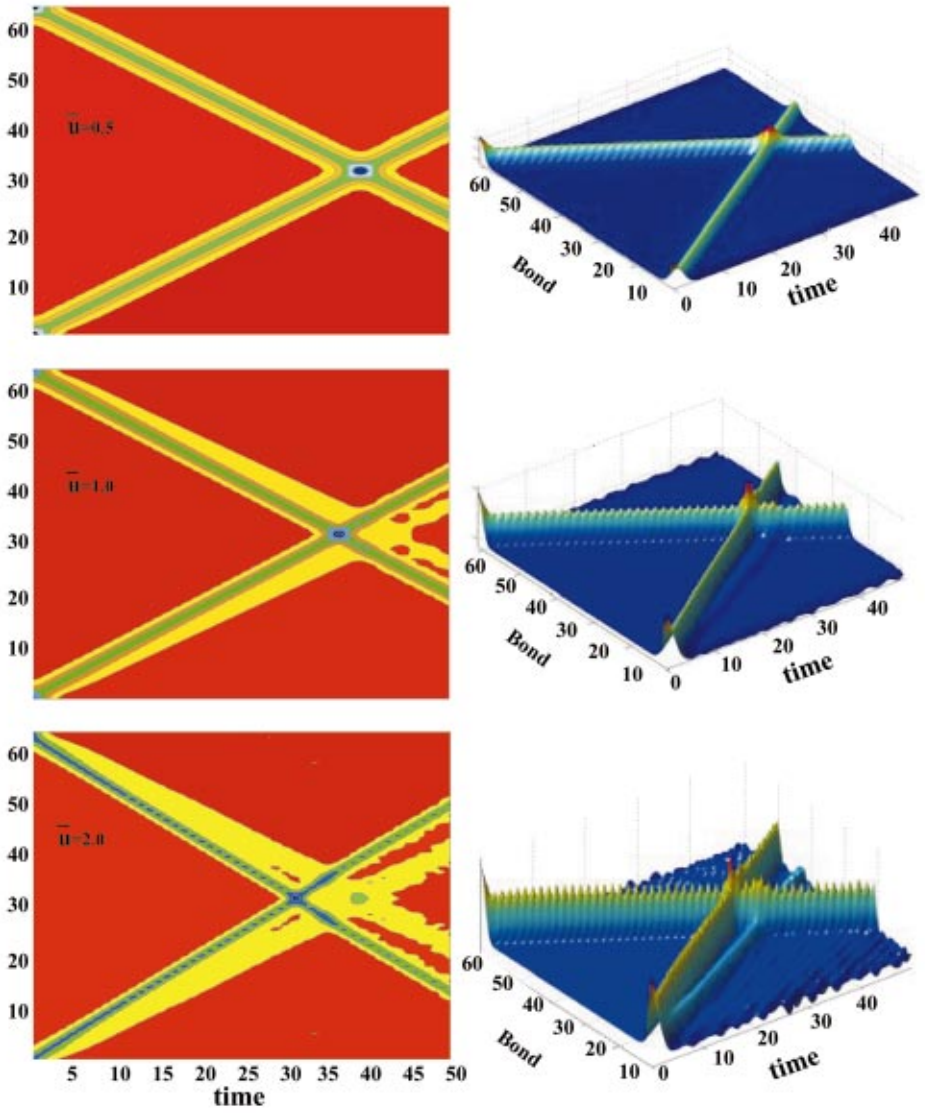

FIG. 5. (Color) TDSCF compression wave for 64 particles for $\bar{u}=0.5$ top and $\bar{u}=1$ middle and $\bar{u}=2$ bottom. The increase in group velocity with amplitude is apparent. An accompanying acoustical wave is clearly seen for the $\bar{u}=2$ case.

It is also found that the full-CI result is faster than the classical and TDSCF result.

Figure 8 is analogous to Fig. 4, but for a higher value of $\hbar(2)$. Two interesting points are first that the soliton seems to survive longer for the more quantum case ($\hbar=2$); this may be a result of the fewer quantum states that the soliton can break up into. Another interesting aspect is that the soliton seems to regenerate itself a long-time after breaking up. This phenomena was persistent in all convergence tests. It could be analogous to another regeneration phenomena in quantum dynamics, partial regeneration of quantum wave packets.[16]

IV. DISCUSSION

In this work we studied the properties of quantum solitons in vibrational systems. Several interesting aspects emerged:

First, solitary-like compression waves were shown to persist for many collisions in a vibrational systems coupled by anharmonic force fields. Due to the exponential growth in computation time the study was limited to a small chain in the quantum regime with effective low mass or high $\hbar$. Nevertheless based on the current calculations it seems that a compact compression wave would propagate at least 100 bonds and may show revival of amplitude further down the chain.

Next, TDSCF, classical and fully-correlated results showed similar trends in the speed-amplitude relations, and the locally based TDSCF shows a slower group velocity of the compression wave. This suggests that locally based mean field approximations[7] are not good enough models for quantum dynamics.

These results can be extended in several directions. First, the nonlinear speed-amplitude relation makes it possible to imagine applications whereby a chirped pulse on, e.g., a chromophore, is used to launch a soliton in which the excitation reaches a specific atom by a shock-wave mechanism (i.e., all the excitation would reach a specific atom in tandem). Thus, soliton-based cleavage can be imagined.

A second possible application is towards planning algorithms whereby one seeks to study, e.g., distances between chromophores. By launching a wave packet from one site, and timing its arrival at another site (at which point the other

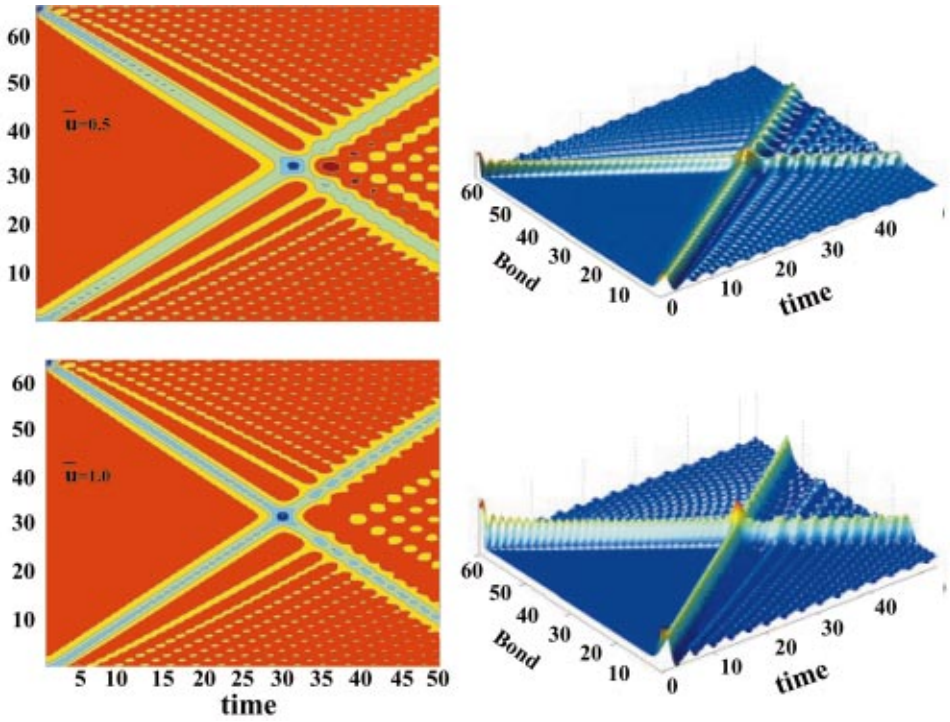

FIG. 6. (Color) Classical compression wave for 64 particles for $\bar{u}=0.5$ top and $\bar{u}=1$ bottom. The main compression waves are followed by weaker acoustical waves with constant group velocity.

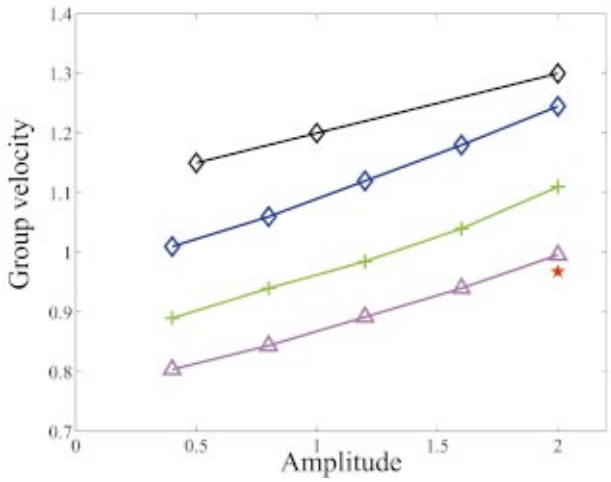

FIG. 7. (Color) Amplitude vs group velocity for the classical and TDSCF compression wave propagation with different values of $\hbar$. Black classical, blue TDSCF $\hbar=2$, green TDSCF $\hbar=1$, pink TDSCF $\hbar=0.5$.

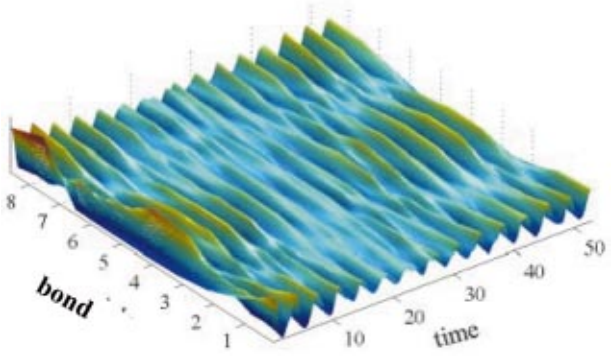

FIG. 8. (Color) Full CI compression wave with effective $\hbar=2$ for nine particles.

chromophore can, e.g., increase its oscillation), the distance between the chromophores can be studied, as well as the elastic properties of the material in-between.

ACKNOWLEDGMENTS

This research was supported by the Israel Science Foundation administered by the Israel Academy of Science and the U.S. National Science Foundation. The Fritz Haber Research Centers is supported by the Minerva Gesellschaft für die Forschung, GmbH München, Germany.

[1] E. Fermi, J. R. Pasta, and S. M. Ulam, "Studies in Nonlinear Problems," Los Alamos Scientific Laboratory Report No. LA-1940, 1955; also in collected works of *Enrico Fermi* (University of Chicago Press, Chicago, 1965), Vol. II, p. 978.
[2] M. Toda, J. Phys. Soc. Jpn. **22**, 437 (1967).
[3] J. Dancz and S. A. Rice, J. Chem. Phys. **67**, 1418 (1977).
[4] T. J. Rolfe, S. A. Rice, and J. Dancz, J. Chem. Phys. **70**, 26 (1979).
[5] M. A. Collins and S. A. Rice, J. Chem. Phys. **77**, 2607 (1982).
[6] M. A. Collins, Adv. Chem. Phys. **53**, 225 (1983).
[7] A. S. Davidov, J. Theor. Biol. **38**, 559 (1973).
[8] A. Scott, Phys. Rep. **217**, 1 (1992).
[9] L. Salasnich, A. Parola, and L. Reatto, Phys. Rev. A **65**, 043614 (2002).
[10] D. Yagi and T. Kawahara, Wave Motion **34**, 97 (2001).
[11] D. Bonart, T. Rössler, and J. B. Page, Physica D **113**, 223 (1998).
[12] R. Kosloff and H. Tal-Ezer, Chem. Phys. Lett. **127**, 223 (1986).
[13] H. Tal Ezer and R. Kosloff, J. Chem. Phys. **81**, 3967 (1984).
[14] R. Kosloff and C. Cerjan, J. Chem. Phys. **81**, 3722 (1984).
[15] Rob H. Bisseling, Ronnie Kosloff, Robert B. Gerber, Mark A. Ratner, L. Gibson, and C. Cerjan, J. Chem. Phys. **87**, 2760 (1987).
[16] I. S. Averbukh and N. F. Perelman, Zh. Eksp. Teor. Fiz. **96**, 818 (1989); Acta Phys. Pol. A **78**, 33 (1990).